Supporting Information for "Enhanced NMR discrimination of pharmaceutically relevant molecular crystal forms through fragment-based ab initio chemical shift predictions"

by J. Hartman, G. Day, and G. Beran

September 21, 2016

Contents

Sections 1–3 in this supporting info provide complete tables of the experimental and predicted chemical shifts used for each polymorphic crystal system. ^{13}C chemical shifts are reported on the neat TMS magic angle spinning scale, and ^{15}N chemical shifts are reported on the solid NH_4Cl scale. Additional details and conversions between scales are discussed in the Supporting Information of Reference [1]. Comparison of the experimental and optimized crystal structures and analysis of the intra- and intermolecular contributions to the chemical shielding are also provided. CIF files containing the optimized geometries of all crystals are provided separately.

1 Acetaminophen

The experimental ^{13}C and ^{15}N chemical shifts for acetaminophen used here were first reported in Ref [2]. Based on private communications with those authors, the referencing of the spectra reported there were corrected using new measurements on form I. Specifically, the original reported ^{15}N isotropic shifts from Ref [2] were shifted by +22.84 ppm to obtain properly referenced isotropic shifts on the neat nitromethane scale. These values were then converted to the solid NH_4Cl scale as previously described.[1]

Similarly, the revised form I ^{13}C resonances were shifted by +0.50 ppm relative to those published in Ref [2]. This correction reduces the discrepancy between the ^{13}C shifts from Ref [2] and those reported in Ref [3] from ∼0.9 ppm to ∼0.3–0.4 ppm. These referencing corrections from form I were then applied to forms II and III.

Table S1: Experimental and predicted isotropic ^{13}C and ^{15}N chemical shifts for acetaminophen forms I, II and III. Predicted shifts are reported using the 2-body, cluster, and combined cluster/2-body models with charge embedding using the PBE0 density functional and both fragment and GIPAW calculations using the PBE density functional (in ppm). The raw chemical shieldings can be obtained from the empirically scaled chemical shieldings reported here using the linear regression parameters reported previously[1] ^{13}C and ^{15}N shieldings are reported relative to TMS and NH_4Cl(s), respectively.

	Exp. Shifts Isotropic	PBE0 2bd 6 Å	PBE0 Cluster 4 Å	PBE0 C/F	PBE 2bd 6 Å	PBE GIPAW
Form I						
C1	132.62	130.75	130.68	130.96	130.25	130.87
C2	123.06	123.69	122.85	123.25	122.43	122.31
C3	115.34	115.75	114.41	114.71	114.41	113.66
C4	151.95	151.69	151.87	151.59	153.14	153.47
C5	116.08	115.30	116.25	115.74	114.09	114.31
C6	120.27	119.94	120.84	120.43	118.50	118.95
C7	169.41	169.32	169.56	169.61	166.76	166.43
C8	23.45	23.83	24.27	24.05	19.50	18.90
N1	97.91	99.68	102.06	101.46	102.60	103.90
Form II						
C1	131.58	129.56	129.55	129.46	129.22	129.69
C2	120.21	120.63	120.28	120.15	119.27	119.27
C3	117.12	118.55	117.21	117.50	117.70	116.13
C4	153.17	153.95	154.03	154.31	155.39	155.36
C5	118.40	118.14	118.20	118.30	117.21	116.92
C6	120.21	120.28	120.72	120.59	119.13	119.54
C7	170.57	171.04	170.69	170.66	168.70	168.13
C8	25.08	27.45	27.05	27.01	23.56	22.05
N1	98.31	102.05	103.99	103.98	104.88	106.02
Form III						
C1	131.14	129.80	129.24	129.40	129.24	129.26
C2	124.79	125.64	125.98	125.64	124.36	123.83
C3	118.25	118.58	119.05	118.40	117.53	116.78
C4	151.94	151.39	152.37	151.76	152.81	153.26
C5	118.25	117.03	116.76	116.72	116.20	116.75
C6	123.18	122.28	122.13	122.38	121.00	122.34
C7	170.00	170.49	170.28	170.27	168.04	167.60
C8	24.34	27.16	27.09	26.94	23.39	22.26
N1	96.31	101.19	102.40	102.05	104.32	105.15
C1'	131.14	128.51	128.34	128.27	127.92	128.55
C2'	124.79	124.21	125.01	124.34	122.90	122.95
C3'	118.25	117.88	118.99	118.18	116.85	116.18
C4'	153.02	153.53	153.88	153.60	154.90	154.75
C5'	118.25	117.78	117.10	117.43	116.91	116.99
C6'	123.18	123.47	122.43	122.93	122.30	122.91
C7'	170.00	169.88	169.55	169.62	167.26	167.35
C8'	24.34	25.79	25.33	25.19	21.88	20.45
N1	95.01	98.35	99.40	99.52	101.15	102.29

2 Phenobarbital

Table S2: Experimental and predicted isotropic ^{13}C and ^{15}N chemical shifts for phenobarbital forms II and III. Predicted shifts are reported using the 2-body, cluster, and combined cluster/2-body models with charge embedding using the PBE0 density functional and both fragment and GIPAW calculations using the PBE density functional (in ppm). The raw chemical shieldings can be obtained from the empirically scaled chemical shieldings reported here using the linear regression parameters reported previously[1] ^{13}C and ^{15}N shieldings are reported relative to TMS and NH_4Cl(s), respectively.

	Exp. Shifts Isotropic	PBE0 2bd 6 Å	PBE0 Cluster 4 Å	PBE0 C/F	PBE 2bd 6 Å	PBE GIPAW
Form IIA						
C1 – Carbonyl	147.15	147.53	147.44	147.53	146.65	146.20
C2 – Ispo	136.00	133.02	135.46	135.30	133.86	137.34
C3 – Quaternary	61.68	63.50	63.27	63.31	64.50	63.96
C4 – Methylene	30.35	33.78	33.91	33.91	32.66	32.34
C5 – Methyl	6.86	8.67	8.67	8.73	3.92	3.70
C6 – CO (edge)	177.41	179.70	179.86	179.92	179.93	180.05
C7 – CO	177.41	178.30	177.74	177.89	178.20	177.96
C8 – Ortho (edge)	125.76	125.02	126.38	126.39	123.93	126.10
C9 – Meta (edge)	131.39	131.12	130.85	131.04	131.12	131.12
C10 – Para	132.41	133.08	132.20	132.44	132.72	132.48
C11 – Meta	132.81	130.19	129.98	130.12	130.02	130.31
C12 – Ortho	129.70	131.72	130.33	130.25	131.98	129.90
N - (edge)	116.13	122.66	123.47	123.63	126.03	127.58
N	111.48	117.20	117.63	117.77	120.36	121.01
Form IIB						
C1 – Carbonyl	148.91	149.43	149.09	149.30	148.34	147.87
C2 – Ispo	137.17	137.54	138.13	137.62	139.22	139.00
C3 – Quaternary	61.00	62.15	62.13	62.19	63.01	62.58
C4 – Methylene	32.21	36.10	36.25	36.14	35.02	34.43
C5 – Methyl	7.93	9.53	9.66	9.65	4.75	4.49
C6 – CO (edge)	169.87	171.61	171.58	171.73	172.21	172.17
C7 – CO	173.20	174.44	174.37	174.48	174.49	174.71
C8 – Ortho (edge)	127.02	127.10	127.21	127.08	126.40	126.94
C9 – Meta (edge)	130.18	130.72	130.49	130.76	130.48	131.05
C10 – Para	129.30	129.32	128.76	129.15	128.52	129.23
C11 – Meta	127.02	126.90	126.75	126.95	126.50	126.94
C12 – Ortho	127.02	128.20	128.20	127.91	127.32	126.89
N – (edge)	113.93	118.85	119.41	119.52	123.00	117.99
N	108.28	112.69	113.59	113.61	115.85	123.99
Form IIC						
C1 – Carbonyl	147.15	147.80	147.76	147.83	147.04	146.42
C2 – Ispo	137.17	137.17	136.64	136.72	139.24	139.08
C3 – Quaternary	62.37	63.46	63.69	63.66	64.69	64.49
C4 – Methylene	27.22	28.74	29.06	29.17	26.32	25.97
C5 – Methyl	8.91	10.47	10.15	10.15	5.68	5.12
C6 – CO (edge)	173.20	175.19	174.87	174.93	175.55	175.04
C7 – CO	174.96	175.79	175.92	175.91	175.52	175.84
C8 – Ortho (edge)	125.40	124.93	124.88	124.86	124.32	124.84
C9 – Meta (edge)	133.74	134.39	134.43	134.37	134.24	134.79
C10 – Para	130.18	131.60	131.20	131.16	130.96	130.78
C11 – Meta	130.18	130.57	130.06	130.04	130.23	129.85

Continued on next page

Table S2 – *Continued from previous page*

	Exp. Shifts Isotropic	PBE0 2bd 6 Å	PBE0 Cluster 4 Å	PBE0 C/F	PBE 2bd 6 Å	PBE GIPAW
C12 – Ortho	125.76	126.52	126.32	126.28	125.63	125.70
N – (edge)	115.15	120.26	120.11	120.27	123.29	123.83
N	109.84	114.72	114.59	114.73	117.67	117.01
Form III						
C1 – Carbonyl	149.01	149.00	149.02	149.13	148.02	147.68
C2 – Ispo	137.56	136.94	136.92	137.00	138.99	139.50
C3 – Quaternary	62.27	63.27	63.29	63.44	64.51	64.00
C4 – Methylene	27.12	28.63	28.87	28.96	26.27	26.08
C5 – Methyl	11.36	12.98	12.86	13.03	8.55	8.21
C6 – CO (edge)	174.20	176.89	176.78	176.92	177.13	177.18
C7 – CO	174.20	175.89	175.67	175.86	175.84	175.72
C8 – Ortho (edge)	127.57	128.12	127.80	127.88	127.70	127.51
C9 – Meta (edge)	130.70	130.29	129.96	129.95	130.33	130.01
C10 – Para	129.53	129.18	129.24	129.28	128.45	128.69
C11 – Meta	129.92	130.93	130.69	130.91	130.66	130.66
C12 – Ortho	127.57	128.26	128.11	128.32	127.32	127.61
N – (edge)	114.50	120.57	120.21	120.35	124.30	123.98
N	108.61	114.37	114.49	114.65	117.55	117.80

3 Testosterone

Table S3: Experimental and predicted isotropic ^{13}C chemical shifts for testosterone. Predicted shifts are reported using the 2-body, cluster, and combined cluster/2-body models with charge embedding using the PBE0 density functional and both fragment and GIPAW calculations using the PBE density functional (in ppm). The raw chemical shieldings can be obtained from the empirically scaled chemical shieldings reported here using the linear regression parameters reported previously[1] ^{13}C and ^{15}N shieldings are reported relative to TMS and NH_4Cl(s), respectively.

	Exp. Shifts Isotropic	PBE0 2bd 6 Å	PBE0 Cluster 4 Å	PBE0 C/F	PBE 2bd 6 Å	PBE GIPAW
$\alpha - U$						
C1	36.19	36.03	35.60	35.59	34.71	33.36
C2	34.55	35.55	35.30	35.28	33.57	33.04
C3	201.22	202.91	202.88	202.85	204.33	205.59
C4	125.67	125.74	126.39	126.32	126.75	126.33
C5	170.64	177.87	175.98	176.24	180.62	181.69
C6	33.76	35.67	35.01	35.02	34.86	33.49
C7	32.40	32.32	32.96	32.95	30.85	32.19
C8	36.92	37.97	36.84	36.83	37.78	35.16
C9	54.14	51.59	52.26	52.27	52.21	54.26
C10	40.03	41.19	40.97	40.98	40.99	40.72
C11	22.99	23.53	24.25	24.25	20.81	20.63
C12	36.78	35.28	36.20	36.21	33.32	34.32
C13	43.67	44.55	43.88	43.87	44.21	42.11
C14	51.14	48.14	50.08	50.08	47.47	50.33
C15	24.33	24.34	24.95	24.92	21.44	21.57
C16	30.19	30.55	30.52	30.46	28.41	27.53
C17	80.35	79.65	79.89	79.87	82.39	82.46
C18	11.67	11.77	11.88	11.88	6.73	6.14

Continued on next page

Table S3 – *Continued from previous page*

	Exp. Shifts Isotropic	PBE0 2bd 6 Å	PBE0 Cluster 4 Å	PBE0 C/F	PBE 2bd 6 Å	PBE GIPAW
C19	18.56	18.49	18.53	18.53	14.37	14.50
$\alpha - V$						
C1	37.20	36.58	36.43	36.40	35.22	34.80
C2	33.76	34.17	34.38	34.34	31.98	31.66
C3	202.72	205.21	205.31	205.22	206.52	207.37
C4	125.17	125.60	125.47	125.48	126.91	125.55
C5	172.09	178.32	176.90	176.95	180.93	183.09
C6	33.50	35.05	35.07	35.01	33.84	33.46
C7	32.25	32.73	32.85	32.76	31.48	31.74
C8	36.44	36.19	36.41	36.37	35.39	34.53
C9	55.26	52.93	52.86	52.82	54.11	54.82
C10	39.57	40.87	41.06	40.99	40.63	40.43
C11	22.02	22.77	22.78	22.77	19.91	19.18
C12	38.41	37.19	37.21	37.23	35.89	35.63
C13	43.57	43.95	44.01	43.98	43.20	42.17
C14	51.86	49.94	50.22	50.21	50.02	50.87
C15	24.23	25.31	25.31	25.27	22.62	21.72
C16	29.86	29.40	29.59	29.58	26.94	26.04
C17	82.69	81.90	81.77	81.80	85.20	85.50
C18	12.21	12.43	12.57	12.57	7.65	6.86
C19	17.92	17.89	17.93	17.89	13.68	13.27
β						
C1	35.25	36.06	36.04	36.20	34.24	34.39
C2	35.25	36.28	36.82	36.63	34.42	34.64
C3	200.15	202.96	203.53	203.21	204.10	199.94
C4	124.65	125.16	125.02	125.12	126.53	127.15
C5	173.75	182.29	182.33	182.08	185.20	181.11
C6	33.45	34.79	35.22	35.29	33.13	33.55
C7	33.45	33.90	34.94	34.94	32.60	33.51
C8	35.25	35.69	35.63	35.66	34.73	33.88
C9	54.65	54.03	54.47	54.38	56.27	54.73
C10	39.35	40.50	41.61	41.46	39.64	39.79
C11	20.95	20.36	22.32	22.18	16.74	19.29
C12	35.25	37.32	37.39	37.33	36.30	35.02
C13	43.55	45.04	45.03	45.00	44.53	42.62
C14	51.55	49.55	51.23	51.09	49.10	50.30
C15	23.95	24.29	25.28	25.23	21.50	21.09
C16	28.75	29.86	28.94	29.00	27.87	26.81
C17	80.65	81.41	81.42	81.40	84.19	84.88
C18	12.55	13.62	13.71	13.73	8.81	7.81
C19	16.85	18.40	18.82	18.81	14.30	15.36

4 Analysis of Optimized Crystal Geometries

Figure S1 presents unit cell overlays between the experimental and relaxed crystal structures. Quantitative root-mean-square deviations in 15-molecule clusters (RMSD15 values) are reported in Table S4, with and without hydrogen atoms. The overlays and RMSD15 values demonstrate generally excellent agreement between the experimental and optimized structures, especially for heavy atoms. Of course, the use of fixed, experimental lattice parameters during the theoretical optimization helps ensure generally good agreement between the two sets of structures.

For acetaminophen forms I and II, only minor deviations (e.g. in the form I methyl group) are observed between the experimental and optimized structures, and RMSD15 values are less than 0.1 Å for non-hydrogen atoms. Slightly larger differences are observed in the orientations of the rings in form III, leading to RMSD15 of 0.15 Å. For phenobarbital, subtle differences can be observed in the angle of the form II phenyl groups at the quaternary carbon, while the two form III structures are in excellent agreement. In α-testosterone, the rings are slightly displaced in the optimized structure relative to the experimental one, but the RMSD15 values are only 0.12 Å. For β-testosterone, the optimized heavy atom positions agree very well with experiment. If one includes hydrogen atoms, the RMSD15 values increase. Of course, hydrogen positions from x-ray diffraction are often unreliable, and in many cases the optimized bond lengths and angles look more reasonable than the experimental ones. In β-testosterone, the orientations of the water molecules also changes somewhat, which contributes to the 0.19 Å RMSD15 value there. In phenobarbital form II, the large 0.25 Å RMSD15 stems from differences in the rotation of the methyl groups and the orientations of the phenyl rings.

We also consider the structural similarities in the individual crystallographically unique monomers, with RMSD values listed in Table S5. RMSD values are $\sim$0.1 Å or less in all cases, with the maximum differences of up to $\sim$0.2 Å.

Table S4: Root-mean-square deviations (in Å) in atomic positions between the experimental and optimized crystal structures as computed in 15-molecule clusters extracted from the crystals (RMSD15[4]).

	non-H Atoms	All Atoms
Acetaminophen:		
Form I	0.092	0.193
Form II	0.072	0.128
Form III	0.153	0.200
Phenobarbital:		
Form II	0.118	0.251
Form III	0.063	0.126
Testosterone:		
α Form	0.117	0.164
β Form	0.061	0.188

Acetaminophen

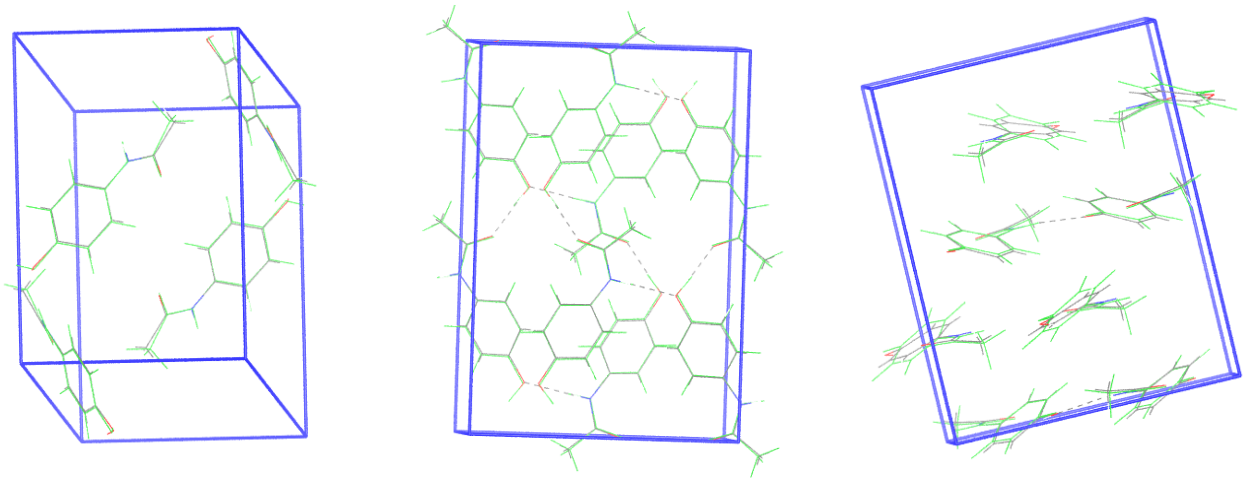

Form I Form II Form III

Phenobarbital

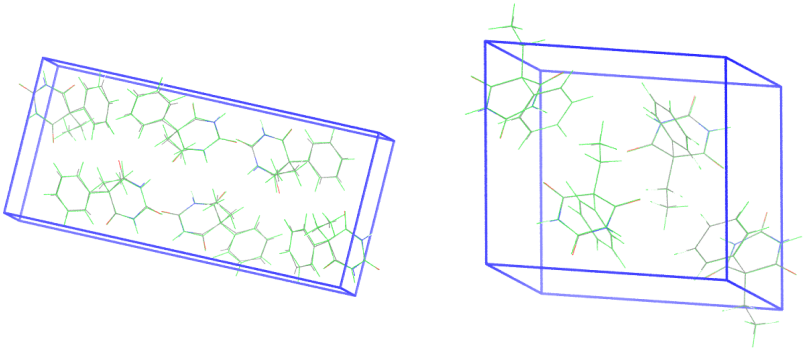

Form II Form III

Testosterone

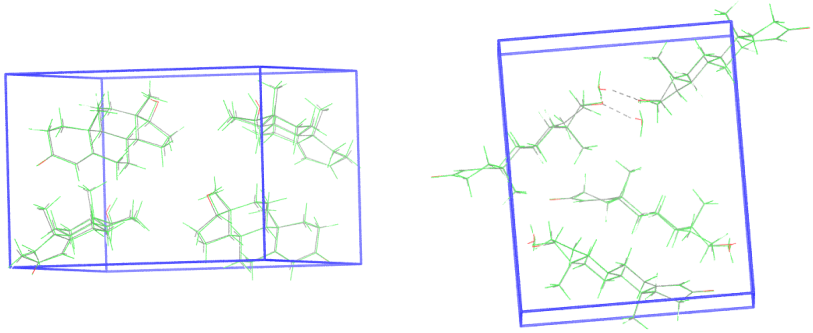

Form II Form III

Figure S1: Overlays of experimental (colored by element) and optimized crystal structures (green).

Table S5: RMSD and maximum deviation for non-hydrogen atom positions (in Å) between the experimental and relaxed crystal structures for each of the crystallographically unique monomers found in the seven crystals considered here.

Crystal	**RMSD**	**Max. Diff.**
Acetaminophen:		
Form I	0.0465	0.0948
Form II	0.0236	0.0412
Form IIIA	0.0281	0.0466
Form IIIB	0.0909	0.1905
Phenobarbital:		
Form IIA	0.1099	0.2031
Form IIB	0.0898	0.1339
Form IIC	0.1102	0.198
Form III	0.0345	0.0625
Testosterone:		
Alpha *U*	0.0311	0.0602
Alpha *V*	0.0318	0.0584
Beta	0.0315	0.0593

5 Intra- and Intermolecular Contributions to Chemical Shielding

The fragment approach allows facile decomposition of the chemical shielding contributions arising from intra and intermolecular contributions. We analyze these features in two ways. First, we computed the chemical shieldings for each isolated, crystallographically-unique monomer (in the same intramolecular conformation as it adopts in the crystal, but with no other molecules or embedding charges around it). This gives the purely intramolecular shielding contributions, $\boldsymbol{\sigma}^{A}_{isolated\ monomer}$. The difference between the isolated monomer shielding for atom A and the full crystalline chemical shielding for the same atom $\boldsymbol{\sigma}^{A}_{crystal}$ (as computed according to Eq 1 in the main paper) corresponds to the intermolecular contribution:

$$\boldsymbol{\sigma}^{A}_{inter} = \boldsymbol{\sigma}^{A}_{crystal} - \boldsymbol{\sigma}^{A}_{isolated\ monomer} \tag{1}$$

To understand the role of intra- versus intermolecular contributions to the differences in shieldings observed among the different polymorphs/crystallographic environments, we then took the difference between for example, the form I and form II acetaminophen intra- and intermolecular shieldings:

$$\Delta\boldsymbol{\sigma}^{A}_{intra}(\text{II}\leftarrow\text{I}) = \boldsymbol{\sigma}^{A}_{intra}(\text{form II}) - \boldsymbol{\sigma}^{A}_{intra}(\text{form I}) \tag{2}$$

$$\Delta\boldsymbol{\sigma}^{A}_{inter}(\text{II}\leftarrow\text{I}) = \boldsymbol{\sigma}^{A}_{inter}(\text{form II}) - \boldsymbol{\sigma}^{A}_{inter}(\text{form I}) \tag{3}$$

Note that the $\Delta\boldsymbol{\sigma}$ notation here simply refers to the change in the shieldings, rather than corresponding to a two-body contribution $\Delta^2\boldsymbol{\sigma}$ of the sort found in Eq 2 of the main paper. These differences were computed for each atom in acetaminophen. Analogous calculations were performed comparing the shieldings on monomers IIIa and IIIb from form III acetaminophen relative to form I. The same procedure was also repeated for phenobarbital form IIa, IIb, and IIc monomers against the form III one, and for αu and αv testosterone monomers relative to the β one. Form III phenobarbital and β-testosterone were chosen simply because they had only a single crystallographically unique monomer in the unit cell ($Z' = 1$). RMS shielding changes are plotted for each case in Figure S2.

From Figure S2, we observe that the changes in chemical shielding arising from intramolecular contributions among the different crystallographic environments are generally smaller than those arising from intermolecular contributions. In other words, while subtle changes in the monomer conformations do affect the chemical shieldings, changes in the intermolecular packing have a larger impact on the chemical shielding variations observed across these different crystal forms.

A second way to analyze the data comes from comparing the discrimination among different potential assignments using an embedded 1-body fragment model instead of the embedded 2-body one advocated in our previous work. Figure S3 presents $\tilde{\chi}^2$ plots for each of the three systems comparing the discrimination achieved by 1-body and 2-body models with both PBE and PBE0. For both acetaminophen and phenobarbital, the RMS errors obtained with the 1-body model are somewhat larger than those obtained with the 2-body one. More importantly, the discrimination among correct and incorrect assignments is notably larger with the 2-body models. For testosterone, the RMS errors for the correct assignment are surprisingly somewhat smaller with the 1-body model than the 2-body one (e.g. 1.75 vs 2.09 ppm for PBE0), but the discrimination is increased with the 2-body model.

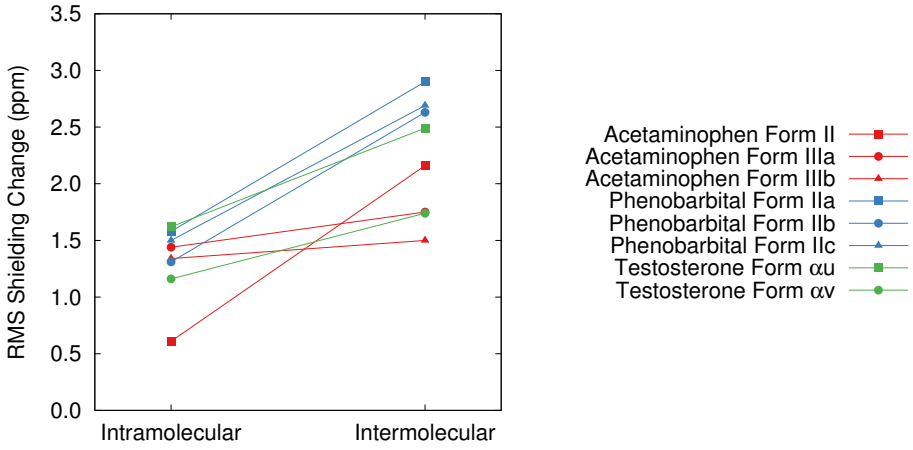

Figure S2: Root-mean-square change in the predicted fragment 2-body PBE0 chemical shieldings (in ppm) from one form to the others, partitioned into intra- and intermolecular contributions. Acetaminophen shieldings were compared against form I, phenobarbital shieldings against form III, and testosterone shieldings against the β form. See text for details.

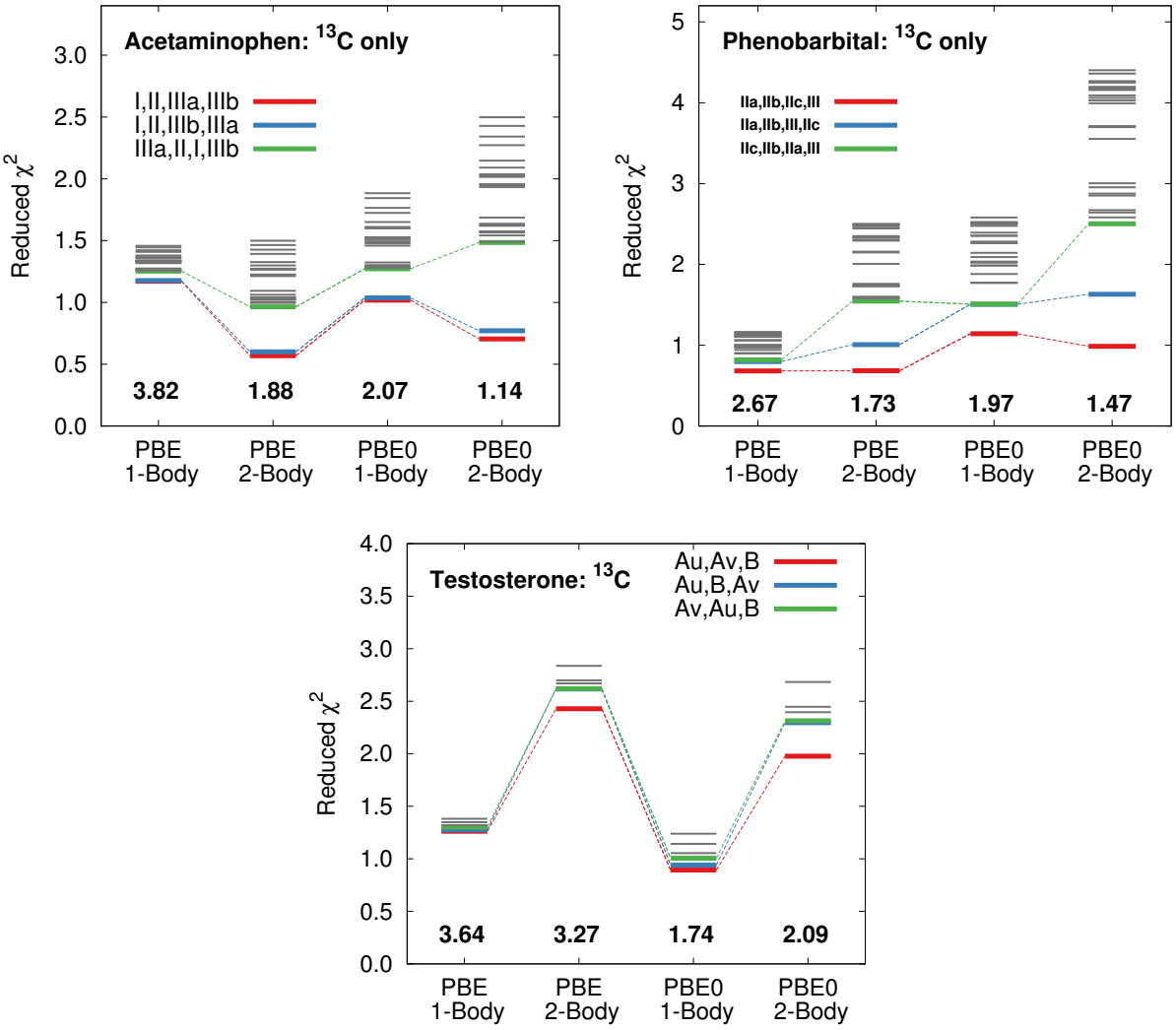

Figure S3: Reduced χ^2 analysis using ^{13}C isotropic shifts illustrating the impact of pairwise contributions on the resolution of difference crystal environments. Results are reported for both the PBE0 and PBE density functionals using all acetaminophen, phenobarbital and testosterone polymorphs.

References

[1] Hartman, J.D., Kudla, R.A., Day, G.M., Mueller, L.J., and Beran, G.J.O. "Benchmark fragment-based ^{1}H, ^{13}C, ^{15}N and ^{17}O chemical shift predictions in molecular crystals." *Phys. Chem. Chem. Phys.*, **18**, 21686–21709 (2016). doi:10.1039/C6CP01831A.

[2] Burley, J., Duer, M., Stein, R., and Vrcelj, R. "Enforcing Ostwald's rule of stages: Isolation of paracetamol forms III and II ." *European J. of Pharm. Sci.*, **31**, 271–276 (2007).

[3] Harper, J.K., Iuliucci, R., Gruber, M., and Kalakewich, K. "Refining crystal structures with experimental ^{13}C NMR shifts tensors and lattice-including electronic structure methods." *Cryst. Eng. Comm.*, **15**, 8693–8704 (2013).

[4] Chisholm, J.A. and Motherwell, W.D.S. "COMPACK: A program for identifying crystal structure similarity using distances." *J. Appl. Crystall.*, **38**, 228–231 (2005). doi: 10.1107/S0021889804027074.